Visible light optical spectroscopy is sensitive to neovascularization in the dysplastic cervix

Vivide Tuan-Chyan Chang
Duke University
Department of Biomedical Engineering
Durham, North Carolina 27708

Sarah M. Bean
Duke University Medical Center
Department of Pathology
Durham, North Carolina 27710

Peter S. Cartwright
Duke University Medical Center
Department of Obstetrics and Gynecology
Durham, North Carolina 27710

Nirmala Ramanujam
Duke University
Department of Biomedical Engineering
Durham, North Carolina 27708

Abstract. Neovascularization in cervical intraepithelial neoplasia (CIN) is studied because it is the precursor to the third most common female cancer worldwide. Diffuse reflectance from 450–600 nm was collected from 46 patients (76 sites) undergoing colposcopy at Duke University Medical Center. Total hemoglobin, derived using an inverse Monte Carlo model, significantly increased in CIN 2+ ($N=12$) versus CIN 1 ($N=16$) and normal tissues ($N=48$) combined with $P<0.004$. Immunohistochemistry using monoclonal anti-CD34 was used to quantify microvessel density to validate the increased hemoglobin content. Biopsies from 51 sites were stained, and up to three hot spots per slide were selected for microvessel quantification by two observers. Similar to the optical study results, microvessel density was significantly increased in CIN 2+ ($N=16$) versus CIN 1 ($N=21$) and normal tissue ($N=14$) combined with $P<0.007$. Total vessel density, however, was not significantly associated with dysplastic grade. Hence, our quantitative optical spectroscopy system is primarily sensitive to dysplastic neovascularization immediately beneath the basement membrane, with minimal confounding from vascularity inherent in the normal stromal environment. This tool could have potential for *in vivo* applications in screening for cervical cancer, prognostics, and monitoring of antiangiogenic effects in chemoprevention therapies.
 [DOI: 10.1117/1.3495730]

Keywords: optical spectroscopy; cervical cancer screening; cervical intraepithelial neoplasia; angiogenesis; immunohistochemistry; microvessel density; hemoglobin quantification.

Paper 10002R received Jan. 3, 2010; revised manuscript received Aug. 12, 2010; accepted for publication Aug. 23, 2010; published online Oct. 7, 2010.

1 Introduction

Among women worldwide, cervical cancer is the third most common cancer with age-standardized incidence rate of 15.3 per 100,000 and mortality rate of 7.8 per 100,000 women.[1] This is largely attributed to the lack of infrastructure and resources in underdeveloped countries to support the organized screening and diagnostic programs that are available to women in developed nations, which consists of Papanicolaou (Pap) smears followed by colposcopy-directed biopsies. Over the last three decades, cervical cancer incidence and mortality rates have decreased ~75% in developed nations, such as the United States,[2] due to effective, albeit costly, early screening and diagnosis of cervical intraepithelial neoplasia (CIN), a premalignant condition. Thus, cervical cancer is preventable and mostly curable if detected early.

To make disease management more cost effective, there is a need to balance the early diagnosis of CIN with the cost and burden of overtreatment. Epidemiologically, high-grade CINs (CIN 2+) are more likely to progress into invasive carcinoma when compared to low-grade CINs (CIN 1), which often spontaneously regress.[3] Thus, the clinically relevant diagnosis is to differentially identify CIN 2+ from normal and CIN 1. Wright et al.[4] recommends continued observation for CIN 1 but immediate treatment for CIN 2+ with excision and ablation. Clinically, pathologists have long relied on cellular morphological changes to diagnose CIN 2+. Of patients with abnormal cytology, only 6–11% will have CIN 2+ and approximately 1 in 1000 will have cervical cancer.[5] The relative insensitivity of conventional cytology means that frequent testing is required for early cancer detection. This is not a practical solution in resource-limited settings, and other solutions are needed. Furthermore, with the declining incidence of CIN in places with wide-scale human papillomavirus (HPV) vaccination programs, such as in the United States, there is an increasing need for an objective diagnosis for CIN 2+ in the face of declining expertise in colposcopy. Other sources of contrast, such as neovascularization, may aid in the early and effective identification of CIN 2+.

The normal cervix is composed of an avascular epithelium and a subjacent vascularized stroma. However, neovascularization (i.e., growth of new blood vessels in areas where blood vessels normally do not exist) can be observed within the epithelium of dysplastic tissues as red patterns of punctuation, or mosaicism, on a white background when viewed

Address all correspondence to: Vivide Tuan-Chyan Chang, Duke University, Department of Biomedical Engineering, Durham, North Carolina 27708; Tel: 919-660-8473; Fax: 919-684-4488; E-mail: vivide.chang@duke.edu

1083-3668/2010/15(5)/057006/9/$25.00 © 2010 SPIE

through a colposcope.[6] The progressively intensifying neovascularization that occurs with increasingly dysplastic CIN is associated with upregulated expression of the vascular endothelial growth factor (VEGF).[6–8] and matrix metalloproteinases, including MMP-9.[9,10] A major HPV oncogene, E6, activates the VEGF promoter and thus mediates neovascularization in the superficial stroma immediately beneath the basement membrane.[11] Although Triratanachat et al.[12] and Leung et al.[13] did not observe an increase in microvessel density (MVD) in CIN 2 (but increased in CIN 3) and CIN 3, respectively, most studies, however, indicate that angiogenesis in the cervix appears to play an important role in the malignant transformation of the cervix.[7] Several groups[7,14,15] have used immunohistochemistry (IHC) to observe neovascularization through increased MVD, or density of small blood vessels having diameters on the order of several red blood cells, in cervical carcinoma. Using factor VIII and CD31, respectively, as immunohistochemical stains for vascular endothelial cells, Abulafia and Sherer[7] and Dellas et al.[16] have also shown that MVD is positively correlated with increasing cervical dysplastic grades. Smith-McCune and Weidner,[17] using anti-factor VIII to target endothelial cells, found no significant difference in neovascularization between CIN 1 and normal controls, yet noted a significant increase in CIN 2+ versus normal controls ($P=0.0006$), and in CIN 2+ versus CIN 1 ($P=0.014$). They have also confirmed the importance of neovascularization in the cervical dysplastic development independent of the degree of associated inflammation. Obermair et al.[6] have shown that neovascularization is correlated with the expression of VEGF in specimens of CIN. In contrast to the ovary and the endometrium, where new blood vessel growth plays an important role in normal physiology, neovascularization in the uterine cervix is primarily a part of the neoplastic process.[7]

Neovascularization is important to quantify for a number of reasons. It plays an important role in tumor progression in the cervix as discussed above.[7,18] Growth of new microvessels in CIN is also a factor associated with poor prognosis and is considered a pathoanatomic feature indicative of a greater risk of recurrence and death.[19,20] Dellas et al.[16] also observed a significant correlation of MVD with overall survival in women with invasive carcinoma and relapse-free survival in patients with regional lymph node metastasis. From a therapeutic perspective, there is a renewed interest in the use of chemopreventive agents for CIN. One such example is the use of highly active antiretroviral therapy (HAART) to prevent opportunistic infections and increased incidence and aggressiveness of certain types of cancer, including cervical cancer in immunocompromised patients.[21,22] Heard et al.[22] have found that direct antitumor effects of HAART may be attributed to inhibition of angiogenesis and tumor growth. Hence, inhibition of neovascularization could serve as a surrogate end point for effectiveness of therapies such as HAART. There is also an interest in establishing a surrogate marker to quantify vascular inhibition and assess the efficacy of antiangiogenic agents at an early stage of disease. Hence, neovascularization is an important parameter to characterize in the uterine cervix.

Characterization of neovascularization has mostly been performed via immunohistochemistry on formaldehyde-fixed and paraffin-embedded tissues using various antibodies.[23] One such antibody is anti-CD34, where CD34 is a trans-membrane glycoprotein constitutively expressed on hematopoietic progenitor cells and endothelial cells.[23] Identification of microvessels typically involves manual selections of regions of interest (ROI) or through automated image analysis algorithms.[24] IHC requires extensive sample processing and is not amenable for *in vivo* measurements. Thus, the development of tools to noninvasively characterize neovascularization changes in the uterine cervix *in vivo* would be of tremendous value. Currently available *in vivo* imaging modalities of blood vessels such as magnetic resonance imaging, computed tomography, positron emission tomography, and singled photon emission computed tomography, require exogenous contrast agents and/or are expensive to perform.[24,25] Doppler ultrasound is not sensitive to blood vessels of $<100\ \mu$m; hence, it is not suitable for quantification of neovascularization.[25] Furthermore, currently there is no effective way to differentiate and measure dysplastic neovascularization immediately below the basement membrane from larger pre-existing vessels in the deep stroma that are part of the normal cervix.

Quantitative visible-light-based optical spectroscopy is inexpensive, portable, and has the potential to be used for *in vivo* quantification of neovascularization changes in soft tissues. Our group has developed a tool consisting of a fast fiber-based spectrometer and a scalable inverse Monte Carlo model to perform quantitative physiology *in vivo*, which has been tested extensively in a laboratory setting[26,27] as well as in preclinical models.[28,29] Using this model, optical absorption and scattering can be quantified, from which total hemoglobin and hemoglobin saturation, as well as tissue scattering due to changes in cellular architecture, can be derived. Furthermore, the sensing depth of the technology can be varied by changing the fiber-optic probe geometry; specifically, by varying the distance between the illumination and collection fibers.

We have previously demonstrated a statistically significant increase in the total hemoglobin concentration *in vivo* in the intact human cervix as it progresses from normal and low-grade dysplasia (CIN 1) to a severely dysplastic state (CIN 2+).[30] However, the study did not provide a validated explanation of the biological basis for this source of optical contrast. In the study reported here, we have quantitatively and systematically compared optical measurements of total hemoglobin concentration to MVD quantified via IHC within the same sites across normal cervical tissues, CIN 1, and CIN 2+. The concomitant increase in MVD and total hemoglobin content in CIN 2+ indicate that quantitative visible-light-based spectroscopy measurements of hemoglobin concentration is primarily sensitive to early neovascularization changes immediately beneath the basement membrane, which is commensurate with the progression of cervical dysplasia. This finding does not appear to be confounded by pre-existing vasculature that is present in the stroma.

2 Method

2.1 *Protocol Design*

The optical spectroscopy and IHC protocols were reviewed and approved by the Institutional Review Board at Duke University Medical Center (DUMC) in accordance with assurances filed with and approved by the Department of Health and Human Services. Informed written consent was obtained

Table 1 Consensus pathology results for optical spectroscopy.

				Excluded		
Tissue type	No. of sites	No. included	Percent included (%)	Motion artifact	Ungradable tissue	Non-CIN
Colposcopic normal squamous[a]	36	36	100	0	0	0
Biopsy-confirmed normal squamous	14	12	86	1	1	0
CIN 1	18	16	89	1	1	0
CIN 2+	16	12	75	3	1	0
Other tissue types[b]	5	0	0	0	0	5
Total	89	76	85	5	3	5

[a]Colposcopically normal squamous sites were not biopsied to maintain the standard of care.
[b]Other tissue types include normal columnar ($N=4$) and flat condyloma ($N=1$), which are excluded from analysis.

from patients referred to the DUMC Colposcopy Clinic following an abnormal Pap smear prior to enrollment in the study. Optical spectra were collected from 89 sites in the cervical transformation zone of 46 female patients age 18–34 (mean ± SD: 24.7 ± 4.4 years). Pregnant women were excluded from the study, and all recruited patients were premenopausal. No invasive squamous cell carcinoma or glandular lesions were identified in this cohort.

Consensus pathology results for optical spectroscopy study are listed in Table 1. Thirteen sites were excluded due to the presence of other tissue types ($N=5$), motion artifacts ($N=5$), and ungradable biopsies ($N=3$). A summary of the consensus pathology results for CD34 study is shown in Table 2. A total of 69 tissue specimens were immunostained, of which 18 sites were excluded due to insufficient tissue for analysis ($N=9$), severely fragmented specimens ($N=7$), and denuded stroma ($N=2$).

2.2 *Optical Spectroscopy*

Details of the optical spectroscopy instrumentation[30] and algorithm[26,27] have been previously described in detail. Briefly, two spectrometers were used in this clinical study: a custom-built spectrometer (instrument A) and SkinSkan® (instrument B) (both from JY Horiba, Edison, New Jersey) with spectral resolutions of 10 and 3.5 nm, respectively. The integration time was set to 100 ms for both instruments, and spectral acquisition took approximately 200 ms and 3 s on instruments A and B, respectively. A bifurcated fiber-optic probe (RoMack, Williamsburg, Virginia) was used to collect diffuse reflectance. The common end that is in contact with tissue consists of a central bundle of 19 illumination fibers, encircled by a ring of 18 collection fibers with a mean source-detector separation 625 μm. All fibers are multimode

Table 2 Consensus pathology results for CD34 IHC.

				Excluded		
Tissue type	No. of sites	No. included	Percent included (%)	Insufficient tissue	Fragmented specimen	Denuded stroma
Biopsy-confirmed normal squamous	24	16	67	4	3	1
CIN 1	30	21	70	4	4	1
CIN 2+	15	14	93	1	0	0
Total	69	51	74	9	7	2

(200/240 μm core/cladding diameter) and have a numerical aperture of 0.22.

Diffuse reflectance spectra for wavelengths (λ) between 450 and 600 nm were collected from colposcopically normal and abnormal sites from patients suspected to have cervical lesions *in vivo*. To account for the wavelength-dependent throughput of the system and drifts in lamp intensity, the raw diffuse reflectance spectrum was calibrated through division by reflectance from a reflectance standard (Spectralon, LabSphere, North Sutton, New Hampshire). Total hemoglobin concentration ([total Hb]) was quantified using a scalable inverse Monte Carlo model[26] from the measured reflectance spectrum.[26] Biopsies from colposcopically abnormal sites were obtained and stained with hematoxylin and eosin for histopathology. Biopsies were then adjudicated by two board-certified pathologists with gynecological expertise, with the adjudicated tissue grade considered to be the standard for comparison. The sensing depth of the fiber-optic probe, defined as the maximum depth that 50% of the detected photons ever penetrated, was evaluated using Monte Carlo simulations as reported in Ref. 30. On the basis of the definition provided above, the mean sensing depth for λ between 450 and 600 nm was 500–600 μm, respectively, which is in the superficial stroma as the average cervical epithelium thickness is 200–500 μm.[31]

2.3 *IHC Study*

Cervical dysplastic neovascularization was assessed through anti-CD34 staining according to a protocol optimized through a retrospective study[32] of 100 cervical biopsies. Vieira et al.[23] have compared three different monoclonal antibodies—anti-CD34, BNH9, and CD31—and concluded that anti-CD34 had higher sensitivity than anti-CD31 and BNH9 in identifying neovascularization in the dysplastic cervix. IHC for CD34 was performed using a semi-automated machine (Dako S3400; Dako, Glostrup, Denmark). Five-micron formalin-fixed paraffin-embedded human cervical biopsy sections were obtained from the cell blocks and were deparaffinized. Antigen retrieval was performed in a steamer for 20 min in antigen-retrieval buffer from the manufacturer. Immunostaining was performed using a modified streptavidin-biotin–horseradish peroxidase technique. The sections were incubated with anti-CD34 (clone: 581; dilution:1:20; BD Biosciences, San Jose, California) for 45 min at 37 °C. The chromogen diaminobenzidine tetrachloride was used to visualize the antibody-antigen complex. Appropriate negative controls, consisting of tissue sections of each case processed with mouse IgG antibody, were prepared along with positive tissue control sections (human tonsil). After immunostaining, the slides were counterstained with hematoxylin, dehydrated in graded alcohols, and mounted on glass slides for digital photomicrograph capture.

2.4 *Microvessel Density Quantification*

Slides were viewed on a multiobserver microscope (DX-50, Olympus, Center Valley, Pennsylvania) with a digital camera (DS-Fl1, Nikon, Melville, New York). Microvessels, defined as vessels with small and usually collapsed or slitlike lumina, with cytoplasmic/luminal CD34 reactions were considered positive for neovascularization. Large and dilated vessels with a lumen larger than ~5 red blood cells and those with muscular walls were excluded because they were not part of dysplasia-induced neovascularization. Areas of greatest MVD (i.e., hot spots) were identified at low power (40×) by a board-certified anatomical pathologist with gynecological specialty expertise (SMB). Hot spots were defined as areas with greatest CD34-reactive vasculature within intact cervical stroma and immediate adjacent epithelium. Subsequently, all CD34-reactive microvessels within a single high power field (400×) were counted and recorded. According to Weidner,[33] any endothelial cell or endothelial cell cluster that was clearly separate from adjacent microvessel and connective tissue elements was considered a single, countable microvessel. Partially identified vessels not completely contained in the field of view were included in the microvessel count. Confounding factors, such as tissue specimen quality, tangential cuts, denuded stroma, nonspecific staining, as well as the degree of inflammation, were quantified using an ordinal scale (negligible/low, medium, and high) and used for quality control purposes. Images with excessive nonspecific staining or extremely poor specimen quality were excluded from the analysis. Two observers (SMB and VTC), blinded to both the biopsy result and inter-observer results, conducted the microvessel counting. The second observer (VTC) was trained by board-certified pathologist (SMB) by identification of microvessels and large vessels on a separate training set of 10 images. One observer (VTC) also independently quantified large and dilated vessels omitted in the microvessel count and combined the two to obtain a total vessel count.

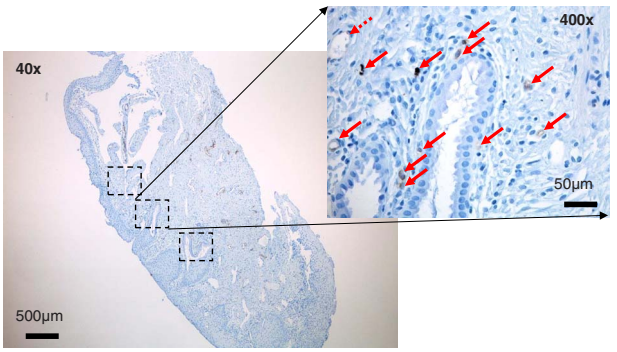

Fig. 1 Selection of up to three hot spots per biopsy specimen (40×). Criteria for admissible hot spots include reactive staining to anti-CD34 and intact epithelium and stroma. In 7 out of 44 specimens, the specimen was too small to select three hot spots; thus, two hot spots were selected instead. Inset: Solid arrows indicate microvessels, and the dashed arrow indicates a large pre-existing vessel with a lumen larger than approximately five red blood cells and hence not included in the microvessel count (400×).

A slide showing the selection of hot spots for microvessel quantification is shown in Fig. 1. The immunostained slide was scanned at low power (10× and 40×) to identify acceptable neovascular hot spots. All microvessel counts were normalized to the same area (~0.72 mm^2) to obtain MVD.

2.5 *Statistical Analysis*

The mean MVD of up to three hot spots per tissue specimen from both observers was used in subsequent analysis. Means from independent quantification of large vessel and total ves-

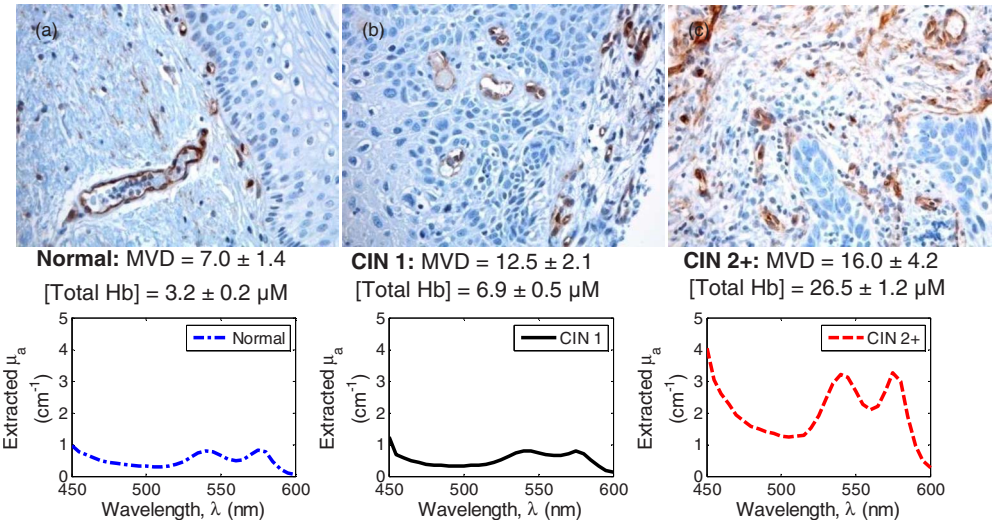

Fig. 2 Photomicrographs of immunostained cervical biopsies and associated optically extracted absorption spectra [$\mu_a(\lambda)$] from representative (a) normal, (b) CIN 1, and (c) CIN 2+ sites, respectively. Vessels with small and usually collapsed, or slitlike, lumina were considered microvessels. Larger vessels with dilated lumen were not included in the MVD quantification. The number of anti-CD34 stained microvessels increases with severity of cervical dysplasia. MVD shown is mean±standard deviation (SD) between two observers. [Total Hb] shown is mean±SD, where SD accounts for uncertainties in data extraction.[30] Concentrations shown represent extracted total hemoglobin content ([total Hb]), which is directly proportional to extracted absorption. Total hemoglobin content is substantially increased in CIN 2+ compared to normal and CIN 1.

sel densities were also used to assess overall vasculature. JMP (SAS, Cary, North Carolina) and MATLAB (MathWorks, Natick, Massachusetts) were used to perform the analysis of variance (ANOVA) to examine intergroup variances, followed by pairwise two-sided Student's t-tests to determine the association of MVD (quantified from IHC) and total hemoglobin content (measured optically) with dysplastic grade. Interobserver variance was assessed through t-tests on the difference between two observers for all valid sites. Reported two-sided P values are considered significant at the $\alpha=0.05$ level. Log-transformed data were used where necessary to approximate normal distributions prior to statistical tests.

3 Results

Representative anti-CD34 stained slides and respective MVD and corresponding absorption spectra $\mu_a(\lambda)$ from 450 to 600 nm and extracted [total Hb], for normal, CIN 1, and CIN 2+ sites from the same two patients are shown in Fig. 2. The CIN 1 and CIN 2+ biopsies were from the same patient while the biopsy-confirmed normal specimen came from a colposcopically abnormal site from a different patient because no colposcopically normal sites were biopsied. There is a marked increase in the area of reactive staining of neovascular microvessels as dysplasia progresses from CIN 1 to CIN 2+. The epithelium also becomes less anisomorphic with an increase in the nuclear-to-cytoplasmic ratio. There is a marked increase in the overall absorption spectrum as dysplasia progresses from CIN 1 to CIN 2+. An increase in both MVD and total hemoglobin concentration was observed with increasing severity of cervical dysplasia.

A summary of the mean and standard error of the mean (SEM) of extracted parameters for different cervical tissue grades is provided in Table 3. Because up to three hot spots per biopsy specimen were quantified, intrapatient and interobserver variations were examined when the minimum, mean, or maximum MVD per specimen obtained by either observer was used exclusively (Table 3). Despite local variations in the number of CD34-reactive microvessels between hot spots and interobserver quantification differences, dysplasia-induced neovascularization changes were preserved and a significantly increased MVD in CIN 2+ versus normal and CIN 1 was observed with all summary measures. Because of interobserver variations, MVD counts obtained by the two observers were significantly different ($P<0.03$, Student's t-test). However, differences in MVD between CIN 2+ and normal and CIN 1 were significant when counts from either observer were used exclusively, $P<0.006$ and $P<0.03$ for observers 1 and 2, respectively (Table 3). To account for interobserver variation and subjectivity in quantifying MVD, mean MVD of all hot spots per specimen obtained by both observers was used in subsequent analysis.

Figure 3 shows the box and whisker plots of mean MVD, extracted [total Hb], mean total vessel density, and mean large-vessel density for all tissue types. The middle line represents the median while the upper and lower edges represent 75 and 25 percentiles, respectively, and crosses indicate outliers. Whereas a statistically significant increase of microvessel density was observed in CIN 2+ versus normal and CIN 1, no significant difference was observed in CIN 2+ for either total vessel or large vessel densities. A concomitant increase in optically extracted [total Hb] was observed in CIN 2+. Using sites (30 sites due to different inclusion criteria) that were common to both CD34 and optical spectroscopy studies, a similarly increased MVD in CIN 2+ versus normal and CIN 1 was observed, whereas no significant differences were observed using either total vessel density or large-vessel density alone (data not shown).

Table 3 Intrapatient and interobserver variations in MVD quantification. MVD values represented as mean ± SEM, where SEM was calculated by dividing sample standard deviation by the square root of the number of biopsies in each tissue type. Minimum, mean, and maximum MVD refer to the lowest, average, and highest microvessel counts, respectively, obtained by each observer per specimen.

Mean ± SEM	Normal	CIN 1	CIN 2+	$P<$
Minimum MVD (observer 1)	7.7 ± 1.3	7.0 ± 1.4	10.0 ± 1.8[a]	0.02
Mean MVD (observer 1)	15.5 ± 1.3	14.5 ± 1.4	20.2 ± 1.8[a]	0.006
Maximum MVD (observer 1)	23.7 ± 1.3	30.3 ± 1.4	34.0 ± 1.8[a]	0.006
Minimum MVD (observer 2)	6.7 ± 1.2	5.5 ± 1.1	10.3 ± 1.7[a]	0.05
Mean MVD (observer 2)	13.3 ± 1.2	14.0 ± 1.1	17.8 ± 1.7[a]	0.03
Maximum MVD (observer 2)	21.3 ± 1.2	26.7 ± 1.1	31.7 ± 1.7[a]	0.05
MVD (mean of observers 1 and 2)	14.0 ± 1.2	14.2 ± 1.2	19.0 ± 1.7[a]	0.007

[a]Statistically a significant difference was observed when comparing CIN 2+ to normal and CIN 1 (collectively) using an unpaired two-sided Student's t-test at the $\alpha = 0.05$ level, with the reported P value.

4 Discussion

Until recently, CIN 1 frequently has been treated to prevent progression to CIN 2+ and eventually to carcinoma of the cervix.[34] However, the current consensus among gynecologists is to view CIN 1 as a normal physiological response to HPV infection that often regresses to normal.[4] This observation is corroborated by the optical and IHC data, where both total hemoglobin and MVD are statistically indistinguishable between normal cervical tissues and CIN 1. However, there is a statistically significant increase of mean MVD in CIN 2+ compared to normal and CIN 1 combined ($P < 0.007$), concordant with the increase in optically extracted [total Hb] of CIN 2+ compared to normal and CIN 1 ($P < 0.004$) combined. Total vessel and large dilated vessel densities were used to infer the degree of vascularization prior to onset of and during dysplastic neovascularization. Because neither was

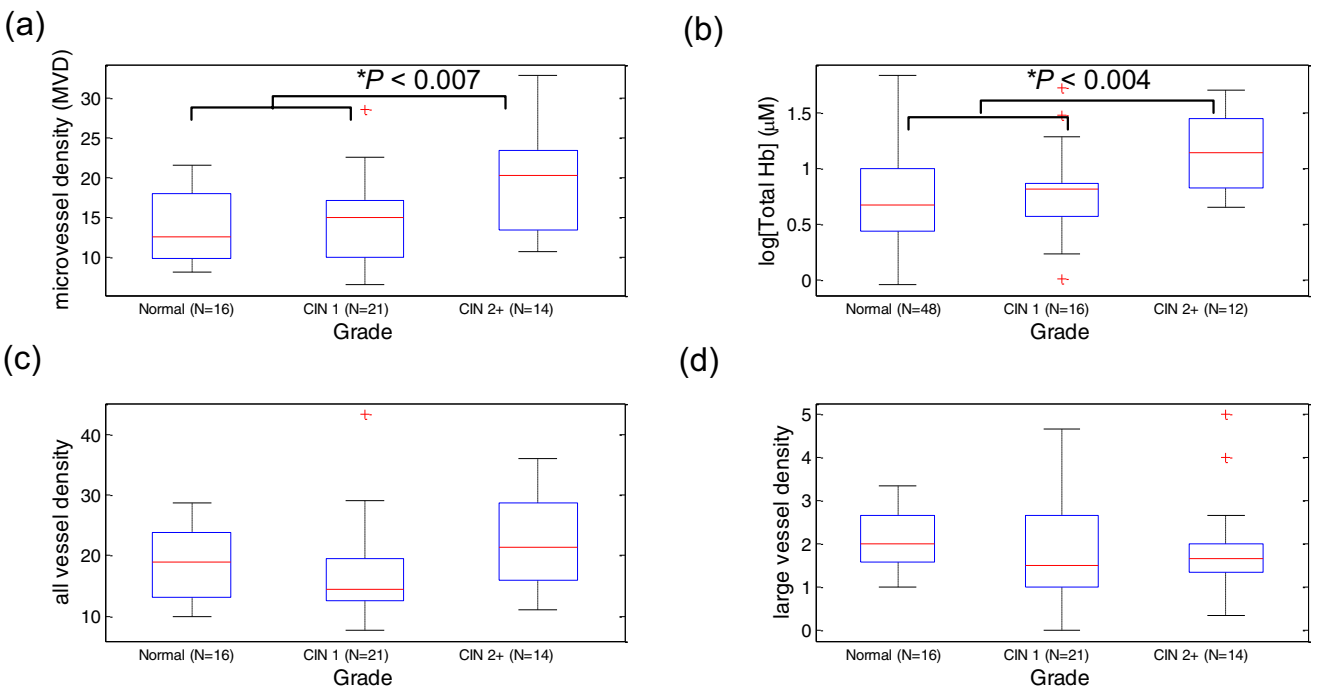

Fig. 3 (a) MVD for different cervical tissue types using all valid IHC sites ($N = 44$). MVD was significantly increased in CIN 2+ compared to normal and CIN 1 combined ($P < 0.007$). (b) Using optical spectroscopy ($N = 76$),[30] [total Hb] is significantly increased in CIN2+ ($P < 0.004$), concordant with the IHC results. Total hemoglobin content was log transformed to satisfy the normality condition in using parametric statistical tests. Both mean MVD and [total Hb] increase in a concordant fashion with increasing severity of cervical dysplasia. (c) Vessel density by including only large nonangiogenic vessels. No significant association between large vessel density and dysplastic grades was observed using ANOVA. (d) Vessel density as calculated by identifying all vessels (microvessel and large nonangiogenic vessels). Similar to large vessel density, no significant association with dysplastic grades was observed using ANOVA.

significantly associated with different CIN grades, dysplastic neovascularization contrast may be masked if the source of contrast included all blood vessels. Various groups[6,16,20,35] have shown that neovascularization in CIN was confined to a narrow zone immediately underneath the dysplastic epithelium and along the basement membrane, whereas the preexisting large vessels part of normal physiology were typically found deeper in the stroma. By tailoring the probe geometry to specifically look at superficial layers of the stroma, it should be possible to quantify neovascularization without the confounding effects of existing vessels.

Utilizing the limited penetration depth of visible light and optimizing the fiber illumination and collection geometry to be sensitive to primarily the epithelial and superficial stromal layers, we were able to preferentially collect photons from just beneath the basal layer. A potentially confounding factor is variation in epithelial thickness between patients. Valadares Guimarães et al.[36] have reported a decrease in epithelial thickness in AIDS patients (HIV status unknown for study patients). However, Walker et al.[31] have shown that epithelial thickness was not correlated with dysplasia status but was dependent on menopausal status. Because all patients recruited for the study were premenopausal, no atrophy of epithelium and corresponding decrease in thickness due to reduction in estrogen level[37] was expected. To address the question of sensitivity to epithelial thickness in instances where this may be an issue, we carried out forward Monte Carlo simulations[38] for a two-layer tissue with cervix-like optical properties.[30,39] The scalable inverse Monte Carlo model developed by our group was used to extract the optical properties from which [total Hb] was derived. Five different epithelial thicknesses (i.e., 200, 300, 350, 400, and 500 μm) spanning the entire range of reported thicknesses in the cervix[31] were used in the simulations to evaluate the sensitivity of the extracted [total Hb] to variations in epithelial thickness. The percent variance in extracted [total Hb] for different thicknesses within this range was found to be $7 \pm 4\%$. Therefore, the absorption contrast observed was minimally impacted by variation in epithelial thicknesses. As previously stated, the sensing depth of the fiber-optic probe used in the study is estimated to be approximately 500 to 600 μm for λ between 450 and 600 nm.[30] Because cervical epithelium averages 200–500 μm in thickness, the fiber-optic probe is designed to be maximally sensitive to photons diffusely reflected from just beneath the basement membrane, where neovascularization occurs. Therefore, optically extracted [total Hb] was less influenced by large vessels in the deep stroma (quantified through the large-vessel density) and more influenced by increased MVD near the basement membrane.

Other optical spectroscopic techniques have been shown to detect neovascularization associated with carcinogenesis in the superficial tissue layer. Using polarization-gating optical spectroscopy, Siegel et al.[40] and Turzhitsky et al.[41] observed an early increase in superficial microcirculation in colon mucosa. Shibuya et al.[42] also observed increased vessel growth and complex networks of tortuous vessels in the bronchial mucosa associated with dysplasia. Another potential confounding factor is the inhomogeneous distribution of hemoglobin absorbers. Finlay and Foster[43] and Lau et al.[44] reported a spectral flattening of hemoglobin absorption spectrum due to pigment packaging, leading to an underestimation of actual hemoglobin concentration. However, Rajaram et al.[45] have shown that inhomogeneity of hemoglobin distribution, such as vessel packing, significantly impact the extraction of absorber concentration if the soret absorption band of hemoglobin is included, but is minimally affected at the α and β absorption bands. If vessel packing is included in the analysis, then we expect our conclusions to remain the same with slightly increased hemoglobin concentration values because our diffuse reflectance data (450–600 nm) do not include the soret absorption band of hemoglobin.

The one-sided Pearson's correlation test showed that MVD and [total Hb] were not significantly correlated (square of Pearson's correlation coefficient, $\rho^2=0.12$, $P<0.19$) when a site by site comparison was made. This is likely attributed to the fact that it is very difficult to precisely match the sample volumes for the two approaches that are being used to measure neovascularization. Furthermore, the choice of hot spots for reactive CD34 staining may not reflect the overall vasculature of the tissue sampled by optical spectroscopy. [Total Hb] was better correlated when the maximum MVD from each specimen was used, with a partially significant $P<0.08$ ($\rho^2=0.21$). Despite these issues, we were able to observe a common underlying phenomenon that led to significant increases in MVD and [total Hb], which arose from neovascularization accompanying cervical dysplastic transformation.

With respect to implementation, optical spectroscopy offers obvious benefits over IHC. Without the need for complex tissue specimen preparation and processing, optical spectroscopy is objective and significantly easier and quicker to implement. Optical spectroscopy can continuously monitor changes in vasculature over time, whereas IHC requires destructive sampling and causes permanent changes to the sampled tissue, while providing only one-time estimates of neovascularization status. The ability to discern neovascularization contrast in CIN 2+ compared to normal and CIN 1 has direct clinical applications in diagnosis and important implications in risk stratification to avoid overtreatment to make cervical precancer screening more cost effective and enable see-and-treat paradigms, which is extremely useful in resource-poor settings. Quantifying the angiogenic microvessels may also predict disease-free status as well as monitor efficacy of anti-VEGF or antiviral therapies. The technology presented can also be modified to access many different organ sites through the use of endoscopes. Furthermore, pathological angiogenesis is not only an exclusive hallmark in cancer, but also in a variety of ischemic and inflammatory diseases.[46] Cells in tumors, wounds, or atherosclerotic plaques become hypoxic when they are too distant from nearby vessels. Coupled with the ability to measure hypoxia,[28] optical spectroscopy may be a suitable tool to monitor the vascular growth and remodeling in numerous disorders.

5 Conclusion

Human anti-CD34 antibody was used to selectively bind to endothelial cells from human cervical biopsies, and MVD was found to increase significantly in CIN 2+ versus normal and CIN 1 ($P<0.007$), concordant with the increase in [total Hb] measured via optical spectroscopy. No statistical significant

difference in MVD was observed between normal and CIN 1. Neither total vessel density nor large-vessel density was significantly associated with dysplastic grade. With the specific fiber geometry used, optical spectroscopy was designed to extract neovascularization contrast confined in a narrow zone immediately beneath the dysplastic epithelium and along the basement membrane. Hence, total hemoglobin content measured through quantitative optical spectroscopy may be used to monitor neovascularization *in vivo*. The validated optical contrast has applications in cervical precancer diagnosis, prognosis, and therapy monitoring for antiangiogenesis or antiviral therapies.

Acknowledgments

The authors acknowledge all the patients who have participated in this study, as well as the staff at DUMC Colposcopy Clinic. The authors also acknowledge Dr. Rex Bentley for consensus pathology and Dr. Zuowei Su for his help with IHC staining. Funding support was provided by NIH Grant No. R21-CA108490-01 and John T. Chambers Fellowship at Duke Fitzpatrick Center for Photonics.

References

1. J. Ferlay, H. Shin, F. Bray, D. Forman, C. Mathers, and D. Parkin, "*GLOBOCAN 2008: Cancer Incidence and Mortality Worldwide: IARC CancerBase No. 10*," International Agency for Research on Cancer, Lyon, France, ⟨http://globocan.iarc.fr⟩ (accessed 20 September 2010).
2. B. J. Monk, M. W. Sill, R. A. Burger, H. J. Gray, T. E. Buekers, and L. D. Roman, "Phase II trial of bevacizumab in the treatment of persistent or recurrent squamous cell carcinoma of the cervix: a gynecologic oncology group study," *J. Clin. Oncol.* **27**(7), 1069–1074 (2009).
3. A.-B. Moscicki, "Human papilloma virus, papanicolaou smears, and the college female," *Pediatric Clinics N. Am.* **52**(1), 163–177 (2005).
4. T. C. Wright, Jr., L. S. Massad, C. J. Dunton, M. Spitzer, E. J. Wilkinson, and D. Solomon, "2006 consensus guidelines for the management of women with cervical intraepithelial neoplasia or adenocarcinoma *in situ*," *Am. J. Obstet. Gynecol.* **197**(4), 340–345 (2007).
5. J. Monsonego, F. X. Bosch, P. Coursaget, J. T. Cox, E. Franco, I. Frazer, R. Sankaranarayanan, J. Schiller, A. Singer, T. Wright, W. Kinney, C. Meijer, and J. Linder, "Cervical cancer control, priorities and new directions," *Int. J. Cancer* **108**(3), 329–333 (2004).
6. A. Obermair, D. Bancher-Todesca, S. Bilgi, A. Kaider, P. Kohlberger, S. Mullauer-Ertl, S. Leodolter, and G. Gitsch"Correlation of vascular endothelial growth factor expression and microvessel density in cervical intraepithelial neoplasia," *J. Natl. Cancer Inst.* **89**(16), 1212–1217 (1997).
7. O. Abulafia and D. Sherer, "Angiogenesis in the uterine cervix," *Int. J. Gynecolog. Cancer.* **10**(5), 349–357 (2000).
8. S. P. Dobbs, L. J. R. Brown, D. Ireland, K. R. Abrams, J. C. Murray, K. Gatter, A. Harris, W. P. Stewart, and K. J. O'Byrne, "Platelet-derived endothelial cell growth factor expression and angiogenesis in cervical intraepithelial neoplasia and squamous cell carcinoma of the cervix," *Ann. Diagn. Pathol.* **4**(5), 286–292 (2000).
9. E. Giraudo, M. Inoue, and D. Hanahan, "An amino-bisphosphonate targets MMP-9-expressing macrophages and angiogenesis to impair cervical carcinogenesis," *J. Clin. Invest.* **114**(5), 623–633 (2004).
10. Y. Zhai, K. B. Hotary, B. Nan, F. X. Bosch, N. Munoz, S. J. Weiss, and K. R. Cho, "Expression of membrane type 1 matrix metalloproteinase is associated with cervical carcinoma progression and invasion," *Cancer Res.* **65**(15), 6543–6550 (2005).
11. O. Lopez-Ocejo, A. Viloria-Petit, M. Bequet-Romero, D. Mukhopadhyay, J. Rak, and R. S. Kerbel, "Oncogenes and tumor angiogenesis: the HPV-16 E6 oncoprotein activates the vascular endothelial growth factor (VEGF) gene promoter in a p53 independent manner," *Oncogene* **19**(40), 4611–4620 (2000).
12. S. Triratanachat, S. Niruthisard, P. Trivijitsilp, D. Tresukosol, and N. Jarurak, "Angiogenesis in cervical intraepithelial neoplasia and early-staged uterine cervical squamous cell carcinoma: clinical significance," *Int. J. Gynecol. Cancer.* **16**(2), 575–580 (2006).
13. K. M. Leung, W. Y. Chan, and P. K. Hui, "Invasive squamous cell carcinoma and cervical intraepithelial neoplasia III of uterine cervix. Morphologic differences other than stromal invasion," *Am. J. Clin. Pathol.* **101**(4), 508–513 (1994).
14. K. Smith-McCune, "Angiogenesis in squamous cell carcinoma *in situ* and microinvasive carcinoma of the uterine cervix," *Obstet. Gynecol.* **89**(3), 482–483 (1997).
15. S. C. Vieira, B. B. Silva, G. A. Pinto, J. Vassallo, N. G. Moraes, J. O. I. Santana, L. G. Santos, G. A. F. Carvasan, and L. C. Zeferinoet al., "CD34 as a marker for evaluating angiogenesis in cervical cancer," *Pathol. Res. Pract.* **201**(4), 313–318 (2005).
16. A. Dellas, H. Moch, E. Schultheiss, G. Feichter, A. C. Almendral, F. Gudat, and J. Torhorst, "Angiogenesis in cervical neoplasia: microvessel quantitation in precancerous lesions and invasive carcinomas with clinicopathological correlations," *Gynecol. Oncol.* **67**(1), 27–33 (1997).
17. K. K. Smith-McCune and N. Weidner, "Demonstration and characterization of the angiogenic properties of cervical dysplasia," *Cancer Res.* **54**(3), 800–804 (1994).
18. O. Abulafia, W. E. Triest, and D. M. Sherer, "Angiogenesis in malignancies of the female genital tract," *Gynecol. Oncol.* **72**(2), 220–231 (1999).
19. W. Tjalma, "Quantification and prognostic relevance of angiogenic parameters in invasive cervical cancer," *Br. J. Cancer* **78**(2), 170 (1998).
20. J. Lee, H. Kim, J. Jung, M. Lee, and C. Park, "Angiogenesis, cell proliferation and apoptosis in progression of cervical neoplasia," *Anal Quant Cytol. Histol.* **24**(2), 103–113 (2002).
21. L. Ahdieh-Grant, R. Li, A. M. Levine, L. S. Massad, H. D. Strickler, H. Minkoff, M. Moxley, J. Palefsky, H. Sacks, R. D. Burk, and S. J. Gange, "Highly active antiretroviral therapy and cervical squamous intraepithelial lesions in human immunodeficiency virus-positive women," *J. Natl. Cancer Inst.* **96**(14), 1070–1076 (2004).
22. I. Heard, J.-M. Tassie, M. D. Kazatchkine, and Gr. Orth, "Highly active antiretroviral therapy enhances regression of cervical intraepithelial neoplasia in HIV-seropositive women," *AIDS* **16**(13), 1799–1802 (2002).
23. S. C. Vieira, L. C. Zeferino, B. B. da Silva, G. Aparecida Pinto, J. Vassallo, G. A. F. Carasan, and N. G. de Moraes. "Quantification of angiogenesis in cervical cancer: a comparison among three endothelial cell markers," *Gynecol. Oncol.* **93**(1), 121–124 (2004).
24. J. R. Garbow, A. C. Santeford, J. R. Anderson, J. A. Engelbach, and J. M. Arbeit, "Magnetic resonance imaging defines cervicovaginal anatomy, cancer, and VEGF trap antiangiogenic efficacy in estrogen-treated K14-HPV16 transgenic mice," *Cancer Res.* **69**(20), 7945–7952 (2009).
25. J. C. Miller, H. H. Pien, D. Sahani, A. G. Sorensen, and J. H. Thrall, "Imaging angiogenesis: applications and potential for drug development," *J. Natl. Cancer Inst.* **97**(3), 172–187 (2005).
26. G. M. Palmer and N. Ramanujam, "Monte Carlo-based inverse model for calculating tissue optical properties. Part I: theory and validation on synthetic phantoms," *Appl. Opt.* **45**(5), 1062–1071 (2006).
27. J. E. Bender, K. Vishwanath, L. K. Moore, J. Q. Brown, V. T. Chang, G. M. Palmer et al. "A robust Monte Carlo model for the extraction of biological absorption and scattering *in vivo*," *IEEE Trans. Biomed. Eng.* **56**(4), 960–968 (2009).
28. J. Q. Brown, L. G. Wilke, J. Geradts, S. A. Kennedy, G. M. Palmer, and N. Ramanujam, "Quantitative optical spectroscopy: a robust tool for direct measurement of breast cancer vascular oxygenation and total hemoglobin content *in vivo*," *Cancer Res.* **69**(7), 2919–2926 (2009).
29. C. Zhu, G. M. Palmer, T. M. Breslin, F. Xu, and N. Ramanujam, "Use of a multiseparation fiber optic probe for the optical diagnosis of breast cancer," *J. Biomed. Opt.* **10**(2), 024032 (2005).
30. V. T. C. Chang, P. T. Cartwright, S. M. Bean, G. M. Palmer, R. C. Bentley, and N. Ramanujam, "Quantitative physiology of the precancerous cervix *in vivo* through optical spectroscopy," *Neoplasia* **11**(4), 325–332 (2009).
31. D. D. C. Walker, B. B. H. Brown, A. A. D. Blackett, J. J. Tidy, and R. R. H. Smallwood, "A study of the morphological parameters of cervical squamous epithelium," *Physiol. Meas* **24**(1), 121–135 (2003).

32. V. T. C. Chang, R. C. Bentley, et al., "Comparison of Chalkley and linear counting techniques for quantification of microvessel density in cervical intraepithelial neoplastic biopsies," (unpublished).
33. N. Weidner, "Intratumor microvessel density as a prognostic factor in cancer," *Am. J. Pathol.* **147**(1), 9–19 (1995).
34. J. T. C. Wright, J. T. Cox, L. S. Massad, J. Carlson, L. B. Twiggs, and E. J. Wilkinson, "2001 consensus guidelines for the management of women with cervical intraepithelial neoplasia," *Am. J. Obstet. Gynecol.* **189**(1), 295–304 (2003).
35. J. L. Burton and M. Wells, "Angiogenesis in gynaecological cancer," *CME J. Gynecol. Oncol.* **5**(2), 156–163.
36. J. Valadares Guimarães, A. K. Marques Salge, D. Silva Gontijo Penha, E. F. Cândido Murta, J. C. Saldanha, E. Costa da Cunha Castro, M. A. dos Reis, and V. de Paula Antunes Teixeira, "Thickness of the cervical epithelium of autopsied patients with acquired immunodeficiency syndrome," *Ann. Diagn. Pathol.* **11**(4), 258–261 (2007).
37. M. Anderson, J. Jordan, A. Morse, and F. Sharp, "*A Text and Atlas of Integrated Colposcopy: For Colposcopists, Histopathologists and Cytologists*," Chapman & Hall, New York (1992).
38. L. Wang, S. L. Jacques, and L. Zheng, "MCML—Monte Carlo modeling of light transport in multi-layered tissues," *Comput. Methods Programs Biomed.* **47**(2), 131–146 (1995).
39. S. K. Chang, D. Arifler, R. Drezek, M. Follen, and R. Richards-Kortum, "Analytical model to describe fluorescence spectra of normal and preneoplastic epithelial tissue: comparison with Monte Carlo simulations and clinical measurements," *J. Biomed. Opt.* **9**(3), 511–522 (2004).
40. M. P. Siegel, Y. L. Kim, H. K. Roy, R. K. Wali, and V. Backman, "Assessment of blood supply in superficial tissue by polarization-gated elastic light-scattering spectroscopy," *Appl. Opt.* **45**(2), 335–342 (2006).
41. V. M. Turzhitsky, A. J. Gomes, Y. L. Kim, Y. Liu, A. Kromine, J. D. Rogers, M. Jameel, H. K. Roy, and V. Backman, "Measuring mucosal blood supply *in vivo* with a polarization-gating probe," *Appl. Opt.* **47**(32), 6046–6057 (2008).
42. K. Shibuya, H. Hoshino, M. Chiyo, K. Yasufuku, T. Iizasa, Y. Saitoh, M. Baba, K. Hiroshima, H. Ohwada, and T. Fujisawa, "Subepithelial vascular patterns in bronchial dysplasias using a high magnification bronchovideoscope," *Thorax* **57**(10), 902–907 (2002).
43. J. C. Finlay and T. H. Foster, "Effect of pigment packaging on diffuse reflectance spectroscopy of samples containing red blood cells," *Opt. Lett.* **29**(9), 965–967 (2004).
44. C. Lau, O. Šćepanović, J. Mirkovic, S. McGee, C.-C. Yu, S. Flughum, Jr., M. Wallace, J. Tunnell, K. Bechtel, and M. Feld, "Re-evaluation of model-based light-scattering spectroscopy for tissue spectroscopy," *J. Biomed. Opt.* **14**(2), 024031 (2009).
45. N. Rajaram, A. Gopal, X. Zhang, and J. Tunnell, "Experimental validation of the effects of microvasculature pigment packaging on *in vivo* diffuse reflectance spectroscopy," *Lasers Surg. Med.* **42**(7), 680–688 (2010).
46. P. Carmeliet and R. K. Jain, "Angiogenesis in cancer and other diseases," *Nature* **407**(6801), 249–257 (2000).